

# Targeted optical fluorescence imaging of human ovarian adenocarcinoma using a galactosyl serum albumin-conjugated fluorophore

Andrew J. Gunn,<sup>1,2</sup> Yukihiro Hama,<sup>1</sup> Yoshinori Koyama,<sup>1</sup> Elise C. Kohn,<sup>3</sup> Peter L. Choyke<sup>1</sup> and Hisataka Kobayashi<sup>1,4</sup>

<sup>1</sup>Molecular Imaging Program, Center for Cancer Research, National Cancer Institute, NIH, 10 Center Drive, Bethesda, MD 20892-1088; <sup>2</sup>Howard Hughes Medical Institute, 4000 Jones Bridge Road, Chevy Chase, MD 20815-6789; <sup>3</sup>Laboratory of Pathology, Center for Cancer Research, National Cancer Institute, NIH, 10 Center Drive, Bethesda, MD 20892-1088, USA

(Received June 4, 2007/Revised July 13, 2007/Accepted July 26, 2007/Online publication September 2, 2007)

Achieving maximal cytoreduction during surgery is a critical prognostic factor for women with advanced-stage ovarian cancer. Targeting optical imaging agents directly to ovarian cancer cells by attaching them to galactosyl (galactosamine-conjugated) serum albumin, whose sugar residues bind surface lectins that are expressed in certain ovarian adenocarcinomas, may improve metastatic tumor identification and resection. Thus, we sought to demonstrate that galactosyl serum albumin-conjugated fluorophores would be a robust mechanism through which to target ovarian cancer by evaluating its tumor-targeting capability in nine human ovarian adenocarcinoma cell lines. The optical fluorophore rhodamine green was conjugated to galactosyl serum albumin, a non-immunogenic targeting molecule. Galactosyl serum albumin-rhodamine green's ability to target nine human ovarian adenocarcinoma cell lines was evaluated by flow cytometry, fluorescence microscopy and *in vivo* optical fluorescence imaging using female athymic nu/nu mice. All nine cell lines tested bound galactosyl serum albumin-rhodamine green more effectively than non-glycosylated controls ( $P < 0.0001$ ). Fluorescence microscopy demonstrated that galactosyl serum albumin-rhodamine green was internalized into each cell line in a galactosamine-dependent manner. *In vivo* optical fluorescence images of intraperitoneal tumor-bearing mice acquired 3 h after intraperitoneal injection of galactosyl serum albumin-rhodamine green successfully differentiated between tumor and normal tissue. This technique also allowed the visualization of submillimeter-sized ovarian tumor implants. These results indicate that galactosyl serum albumin-rhodamine green can selectively target a variety of human ovarian adenocarcinomas for optical fluorescence imaging and thus may improve intraoperative tumor detection and resection. (*Cancer Sci* 2007; 98: 1727–1733)

The majority of women with ovarian cancer have a poor prognosis because they already have advanced-stage disease with peritoneal metastasis at the time of diagnosis.<sup>(1)</sup> Cytoreductive surgery followed by systemic or peritoneal chemotherapy is the standard of care for the initial management of women with advanced-stage ovarian cancer. Optimal tumor debulking, defined as removing all lesions >1 cm in diameter, is an important surgical objective and a critical prognostic factor for patients with ovarian cancer.<sup>(2)</sup> Moreover, reducing the amount of residual disease after cytoreduction to microscopic levels further improves clinical outcomes.<sup>(3,4)</sup> However, cytoreduction is often suboptimal due to the small size and location of the implants and the poor visual contrast between tumor and normal tissue under the white-light conditions typically present in the operating room. One possible approach to improve the resection of tumor implants is to administer a targeted optical fluorophore that binds to ovarian tumors with high affinity and specificity. This type of imaging agent could provide the surgeon with a highly sensitive and specific intraoperative guide to tumor

location that could also identify small peritoneal implants (<1 mm) that would otherwise go undetected by the unaided eye.<sup>(5)</sup>

The  $\beta$ -D-galactose receptor is a surface lectin that is expressed on a variety of cancer cells, including certain types of ovarian cancers.<sup>(6,7)</sup> This receptor functions to bind and internalize glycosylated proteins that contain specific sugar residues.<sup>(8)</sup> Serum albumin can be converted into galactosyl serum albumin (GSA), a ligand for this receptor, through conjugation to lectin-binding galactosamine residues.<sup>(9)</sup> Thus, a GSA-conjugated optical fluorophore may be a clinically useful agent for use during cytoreductive surgery to highlight ovarian tumor implants.<sup>(9)</sup> Herein, we demonstrate the feasibility of this approach in a wide variety of ovarian adenocarcinomas both *in vitro* and *in vivo*.

## Materials and Methods

**Synthesis of GSA-rhodamine green and bovine serum albumin-rhodamine green.** Bovine serum albumin (BSA) and GSA, which has 23 galactosamine residues conjugated to each BSA, were purchased from Sigma Chemical (St Louis, MO, USA) and amido-reactive rhodamine green (RhodG) was purchased from Molecular Probes (Eugene, OR, USA). At room temperature, 400  $\mu$ g of either GSA or BSA in 196  $\mu$ L Na<sub>2</sub>HPO<sub>4</sub> was incubated with 4  $\mu$ L of a 6 mM solution (24 nmol) of RhodG-succinimidyl ester in dimethyl sulfoxide for 15 min. The mixture was then purified with a Sephadex G-50 Gel Filtration System (PD-10; GE Healthcare, Milwaukee, WI, USA). GSA- and BSA-RhodG samples were kept at 4°C as stock solutions.

The protein concentration of GSA- and BSA-RhodG samples was determined with a Coomassie Plus Protein Assay Reagent Kit (Pierce Biotechnology, Rockford, IL, USA) by measuring the absorption at 595 nm with a spectrophotometer (8453 UV-Vis Value System; Agilent Technologies, Palo Alto, CA, USA) using GSA and BSA standards, respectively. The RhodG concentration of both GSA- and BSA-RhodG samples was measured by the absorption at 504 nm using the same spectrophotometer. The number of fluorophore molecules conjugated to each BSA or GSA molecule was determined by dividing the RhodG concentration of each sample by either the BSA protein concentration or GSA protein concentration, respectively. To directly compare the fluorescence intensity of GSA-RhodG to BSA-RhodG, the number of RhodG molecules conjugated to each protein was made approximately equal (approximately three RhodG per BSA or GSA) by adjusting the protein concentration of each sample. Because RhodG continued to fluoresce even after conjugation with GSA or BSA, the paired samples used for

<sup>4</sup>To whom correspondence should be addressed. E-mail: kobayash@mail.nih.gov

*in vitro* and *in vivo* experiments produced almost the same fluorescence emission signals. Finally, in order to validate that the fluorophores were associated with the respective proteins, both conjugates were analyzed by gel filtration using a high-performance liquid chromatography system equipped with an in-line UV detector (System Gold, Beckman Coulter, Fullerton, CA, USA) and fluorescence detector (FP2020; Jasco, Easton, MD, USA) using a TSK G2000 30-cm column (TOSO Bioscience LLC, Montgomeryville, PA, USA) with 0.066 M 1× phosphate-buffered saline (PBS).

**Cell culture.** The following human ovarian adenocarcinoma cell lines were used: SHIN3 (provided by Dr S. Imai, Nara, Japan),<sup>(10)</sup> SKOV3 and CaOV3 (obtained from the American Type Culture Collection, Manassas, VA, USA), A2780 (a gift from Dr T. Fojo, National Cancer Institute, NIH, Bethesda, MD, USA), HEY-A8 (a gift from Dr G. Mills, M.D. Anderson Cancer Center, Houston, TX, USA), and OVCAR4,<sup>(11)</sup> OVCAR5,<sup>(11)</sup> OVCAR8<sup>(11)</sup> and IGR-OV1<sup>(12)</sup> (provided by the Developmental Therapeutics Program, National Cancer Institute-Frederick, NIH, Frederick, MD, USA). SKOV3 was grown in McCoy's 5A medium (Quality Biological, Gaithersburg, MD, USA) containing 10% fetal bovine serum (FBS; Gibco, Gaithersburg, MD, USA) and 1% non-essential amino acids (BioWhittaker, Walkersville, MD, USA). All other cell lines were grown in RPMI-1640 medium (BioWhittaker) containing 10% FBS, 0.03% L-glutamine, 100 U/mL penicillin and 100 µg/mL streptomycin. All cell lines were grown at 37°C in 5% CO<sub>2</sub>.

**Flow cytometry.** Single-color flow cytometry was carried out to evaluate whether the cell lines could bind GSA-RhodG in a galactosamine-dependent fashion. Cells from each line were incubated for 16 h, after which they were either left untreated or had either 3 µg/mL of BSA-RhodG or GSA-RhodG added to the media. After an additional 3 h incubation, the cells were then trypsinized and washed once with 1× PBS. Flow cytometry was carried out immediately using a FACScan cytometer (Becton-Dickinson, Franklin Lakes, NJ, USA). The argon ion 488-nm laser was used for excitation. Signals from cells were collected using a 530/30 nm band-pass filter. All data were analyzed using CellQuest software (Becton-Dickinson, Franklin Lakes, NJ, USA). The percentage of fluorescent-gated cells and mean fluorescence intensity (MFI) is indicated for each experimental condition.

**Fluorescence microscopy.** Fluorescence microscopy was used to demonstrate that GSA-RhodG is internalized by the cells in a galactosamine-dependent fashion. Cells from each line were plated on coverglass-bottom culture wells and incubated for 16 h, after which each well was left untreated or had either 3 µg/mL BSA-RhodG or GSA-RhodG added to the media. After an additional 3 h incubation, the coverglass with attached cells was removed and washed once with 1× PBS. Fluorescence microscopy was carried out using an Olympus BX51 microscope (Olympus America, Melville, NY, USA) with excitation at 470–490 nm and emission at 515 nm long pass. Transmitted light differential interference contrast (DIC) images were also acquired. Images were acquired at 20× magnification with 2 ms exposure for DIC images and 500 ms exposure for fluorescence microscopy images.

**Tumor model.** All animal experiments were carried out in compliance with the Guide for the Care and Use of Laboratory Animal Resources (1996), National Research Council, and approved by the National Cancer Institute Animal Care and Use Committee. The establishment of intraperitoneal (i.p.) tumor xenografts was attempted with each cell line by the i.p. injection of 2 × 10<sup>6</sup> cells suspended in 300 µL 1× PBS into female NIH nu/nu mice (National Cancer Institute Animal Production Facility, Frederick, MD, USA). Tumor xenografts were successfully established with the SHIN3, SKOV3, OVCAR5 and OVCAR8 cell lines. Experiments with tumor-bearing mice were carried out approximately 3 weeks after cell injection.

***In vivo* fluorescence imaging.** Tumor-bearing mice received an i.p. injection of 25 µg of either GSA-RhodG or BSA-RhodG diluted in 300 µL 1× PBS. The mice were killed by CO<sub>2</sub> inhalation 3 h after administration of the agent and the abdominal walls were then removed. White-light photos and spectral fluorescence images of the entire exposed abdomen were obtained using the Maestro In Vivo Imaging System (CRi, Woburn, MA, USA). A loop of bowel and mesentery from each mouse treated with GSA-RhodG was then removed and imaged separately by the same system in order to demonstrate the ability of GSA-RhodG to detect submillimeter-sized ovarian tumor foci. A band pass filter from 445 to 490 nm and a long pass filter over 515 nm were used for excitation and emission light, respectively. The tunable filter was automatically stepped in 10-nm increments from 500 to 800 nm while the camera captured images at each wavelength interval with constant exposure. Commercially available Maestro software with spectral unmixing algorithms was used to create the spectral fluorescence composite images (Nuance version 1.4; CRi).

A direct comparison of the fluorescence intensity of BSA-RhodG-treated and GSA-RhodG-treated tumor xenografts was made by imaging the tumor nodules side-by-side *ex vivo*. A semiquantitative analysis of the two tumor nodules was carried out by drawing a region of interest as large as each tumor to determine the fluorescence intensity using ImageJ software (<http://rsb.info.nih.gov/ij/plugins/mri-analysis.html>). The dynamic range of the fluorescence intensity in arbitrary units (a.u.) was split into 256 equal-sized bins (0–255).

## Results

**Flow cytometry.** The percentage of fluorescent-gated cells, which corresponds to cell binding by either the BSA- or GSA-RhodG conjugate, is shown in Fig. 1. After incubation with GSA-RhodG, the average percentage of fluorescent-gated cells for all cell lines analyzed was 97.7% (range 89.5–99.8%), which was significantly higher than when the cells were incubated with BSA-RhodG (mean 20.7%, range 7.3–32.2%) ( $P < 0.0001$ ). The average MFI for cells incubated with GSA-RhodG was 170.6 (range 74.7–310.9), which was also significantly higher than the average MFI for cells incubated with BSA-RhodG (mean 8.6, range 5.5–10.9) ( $P < 0.0001$ ). The flow cytometry data indicate that all the ovarian adenocarcinoma cell lines tested bind GSA-RhodG in a galactosamine-dependent manner, suggesting that they can be targeted for *in vivo* optical fluorescence imaging by GSA-RhodG.

**Fluorescence microscopy.** After incubation with 3 µg/mL GSA-RhodG, cells from each line demonstrated intracellular fluorescent GSA molecules (Fig. 2a). Although the number and intensity of the fluorescent molecules differed between cell lines, these images confirmed that GSA-RhodG is internalized after binding to the ovarian cancer cells. DIC images are shown in Fig. 2 for orientation. Fluorescence microscopy images were also obtained after incubation with BSA-RhodG; however, none of these images revealed intracellular fluorescent molecules (Fig. 2b).

***In vivo* optical fluorescence imaging.** Successful i.p. tumor xenografts were established with the SHIN3, SKOV3, OVCAR5 and OVCAR8 cell lines. Tumor-bearing mice received an i.p. injection of 25 µg of either GSA-RhodG or BSA-RhodG. Side-by-side *in vivo* spectral fluorescence images of the entire exposed abdomen obtained 3 h after agent injection demonstrated that GSA-RhodG produced a qualitatively higher tumor-associated fluorescence than BSA-RhodG in tumor xenografts of SKOV3 (Fig. 3a), OVCAR5 (Fig. 3b) and OVCAR8 (Fig. 3c). White-light photos of the bowel and mesentery of SKOV3 (Fig. 3d), OVCAR5 (Fig. 3e), and OVCAR8 tumor-bearing mice (Fig. 3f) treated with GSA-RhodG reveal minimal visible tumor implants. Spectral fluorescence composite images of the same tissue,

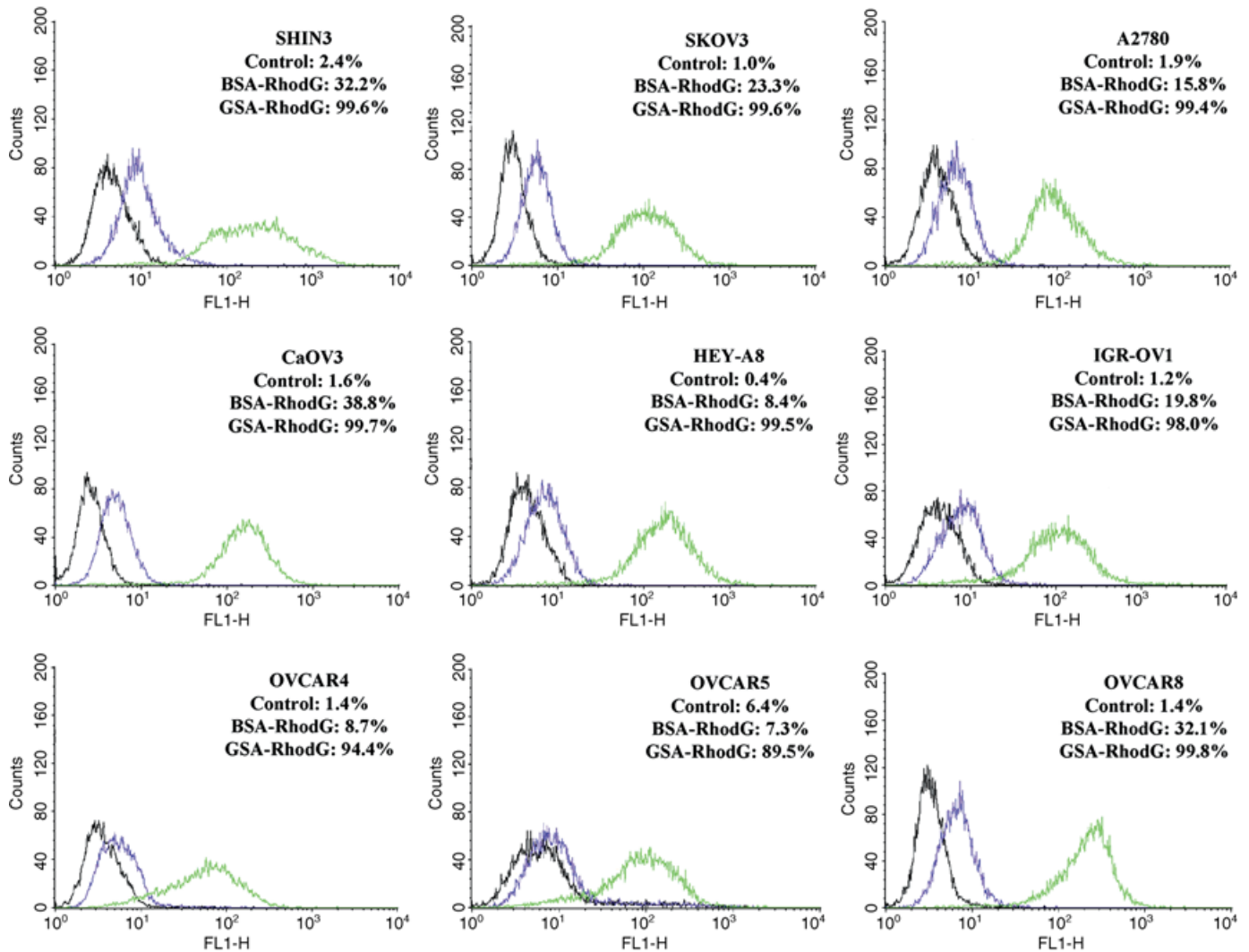


**Fig. 1.** Flow cytometry results from nine human ovarian adenocarcinoma cell lines after incubation with either 3  $\mu\text{g}/\text{mL}$  galactosyl serum albumin (GSA)-rhodamine green (RhodG) (green lines) or bovine serum albumin (BSA)-RhodG (purple lines). Untreated controls (black lines) are also shown. The percentage of fluorescent-gated cells, which corresponds to the number of cells that were labeled by the protein-fluorophore conjugates, is shown for each experimental condition. The percentage of fluorescent-gated cells and mean fluorescence intensity is highest after GSA-RhodG incubation for all nine cell lines.

however, were able to identify numerous submillimeter-sized tumor implants (Fig. 3g-i), thus demonstrating the ability of GSA-RhodG to locate micrometastatic disease. A semiquantitative analysis of tumor fluorescence by ImageJ software (Fig. 4) showed that tumor nodules derived from SKOV3 tumor-bearing mice treated with GSA-RhodG had a higher fluorescence intensity (mean 717) than nodules removed from mice treated with BSA-RhodG (mean 94.4) ( $P < 0.0001$ ). Similar results were obtained for OVCAR5 and OVCAR8 tumor-bearing mice ( $P < 0.0001$  for both data sets). These data reveal that GSA-RhodG targets ovarian tumor xenografts *in vivo* more effectively than non-glycosylated BSA-RhodG.

## Discussion

It was previously unknown whether the optical imaging probe GSA-RhodG could be used to specifically target a wide variety of ovarian adenocarcinomas for intraoperative identification. Thus, the goal of the present study was to evaluate the ability of nine human ovarian adenocarcinoma cell lines to be targeted

*in vitro* and *in vivo* by GSA-RhodG. Analysis by flow cytometry showed that GSA-RhodG bound to all ovarian adenocarcinoma cell lines tested in a galactosamine-dependent manner, whereas fluorescence microscopy documented that these cell lines internalize GSA-RhodG but not the non-glycosylated BSA-RhodG. Moreover, tumor-targeted optical fluorescence imaging with GSA-RhodG successfully identified tumors in three new models of late-stage ovarian cancer, thus extending our laboratory's pilot studies using the SHIN3 cell line<sup>(9)</sup> to a broader spectrum of ovarian adenocarcinomas. These data suggest that tumor-associated lectins are expressed in sufficient quantities on all nine cell lines tested to enable them to act as a general molecular target in ovarian adenocarcinoma for GSA-RhodG. Thus, it is likely that many, if not all, ovarian adenocarcinomas could be targeted for optical imaging using GSA-RhodG.

The administration of a tumor-targeted optical imaging probe such as GSA-RhodG could provide surgeons with an intraoperative guide to tumor location that identifies submillimeter-sized tumor foci that might otherwise go undetected because of their

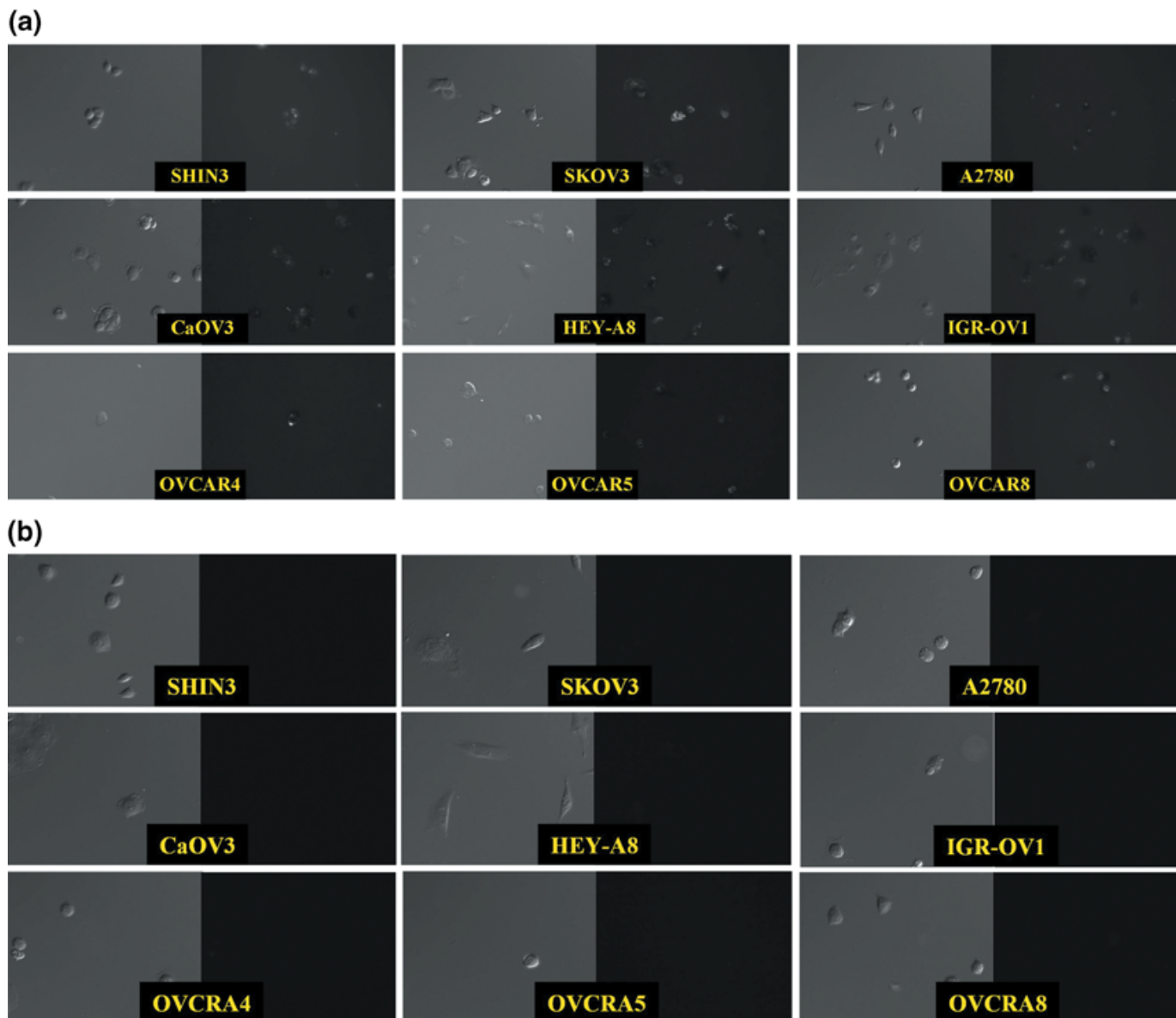


**Fig. 2.** Transmitted light differential interference contrast (DIC) (left) and fluorescence microscopy (right) images from nine human ovarian adenocarcinoma cell lines after incubation with 3  $\mu\text{g}/\text{mL}$  of (a) galactosyl serum albumin (GSA)–rhodamine green (RhodG) or (b) bovine serum albumin–RhodG. The appearance of intracellular fluorescent GSA molecules demonstrates that only GSA–RhodG is internalized by the cells.

small size or unusual location. GSA–RhodG’s favorable pharmacokinetic properties, such as rapid clearance from the peritoneal space and swift hepatic metabolism that prevents recirculation, result in high signal-to-background ratios that make it a particularly attractive imaging probe for peritoneal carcinomatosis. Thus, it is hoped that the advancement of this technology to the clinical realm will ultimately improve survival for women with late-stage ovarian cancer.

The two components of this ovarian tumor-targeted optical imaging probe, RhodG as the optical fluorophore and GSA as the targeting moiety, were selected because of their favorable biological characteristics. The short penetration of green fluorescent dyes in tissue ordinarily limits their use to *in vitro* applications in favor of near-infrared dyes, which have a longer penetration distance. However, when the target is on the surface, green dyes are actually preferable to near-infrared dyes because they are efficient

fluorophores that yield an extremely bright signal (Fig. 4). RhodG was previously determined to be an ideal fluorophore for this type of application because its fluorescence, instead of fading like other green fluorescent probes, actually increases in intensity after internalization by ovarian cancer cells.<sup>(13)</sup> The glycoprotein avidin is a ligand for lectins like the  $\beta$ -D-galactose receptor,<sup>(8)</sup> and has been successfully used as a targeting moiety for the *in vivo* imaging of ovarian adenocarcinomas.<sup>(5,7)</sup> However, its immunogenicity precludes its clinical use.<sup>(14,15)</sup> Thus, in a previous study, our laboratory evaluated GSA as an alternative to avidin because a <sup>99m</sup>technetium-labeled analog is already in clinical use in Japan.<sup>(16)</sup> Indeed, GSA–RhodG proved to be a more effective tumor-targeted optical probe than avidin–RhodG.<sup>(9)</sup>

There are several potential clinical questions that should be considered prior to implementing this technique in humans. First, it is well known that some patients with metastatic ovarian cancer have intra-abdominal adhesions due to prior surgeries or

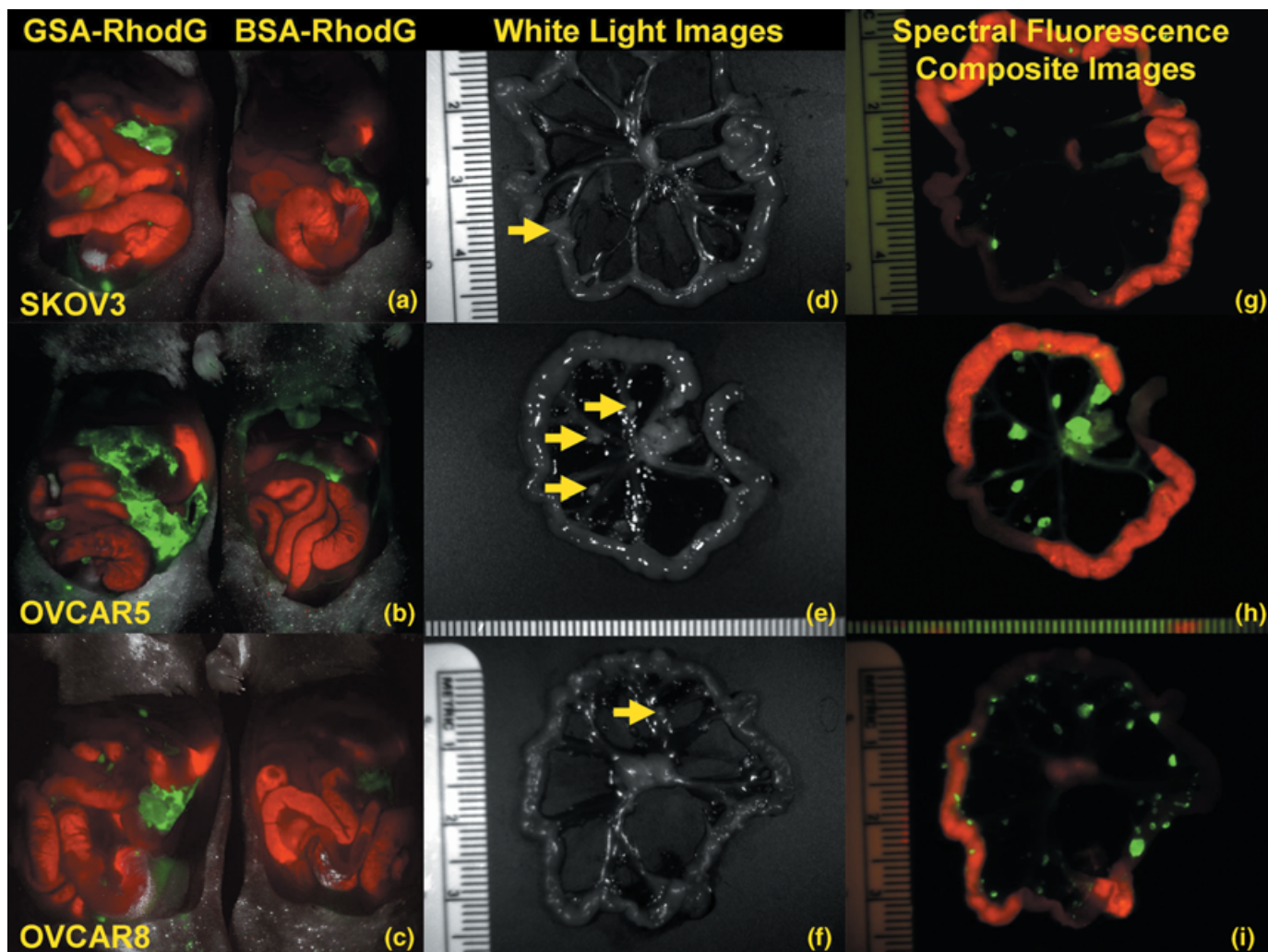


**Fig. 3.** (a) Side-by-side spectral fluorescence composite image of the exposed abdomens of SKOV3 tumor-bearing mice treated with galactosyl serum albumin (GSA)-rhodamine green (RhodG) (left) and bovine serum albumin (BSA)-RhodG (right) demonstrates brighter tumor-associated fluorescence with GSA-RhodG than with BSA-RhodG. (b,c) Similar results were observed for OVCAR5 and OVCAR8 tumor-bearing mice, respectively. (d) White-light photo of a loop of bowel and mesentery from a SKOV3 tumor-bearing mouse treated with GSA-RhodG identifies only one tumor nodule (yellow arrow). (e,f) Similar results were observed for OVCAR5 and OVCAR8 tumor-bearing mice, respectively. (g) Spectral fluorescence composite image of the same tissue shown in 3-D now reveals multiple tumor nodules (green), indicating that targeted optical imaging can identify more disease than the unaided eye. (h,i) Similar results were observed for OVCAR5 and OVCAR8 tumor-bearing mice, respectively. (Note: Red = autofluorescence of the gastrointestinal tract.)

i.p. chemotherapy that could limit the agent's access to all tumor implants. Furthermore, many patients with advanced-stage ovarian cancer have literally thousands of metastases, which makes the resection of all disease, even if made visible by the use of tumor-targeted optical fluorophores, a clinical impracticality. However, this type of imaging probe could have other applications apart from those already described in this report. For example, GSA-RhodG could be administered to patients undergoing surgery for stage I/II ovarian cancer in order to rule out the presence of micrometastatic disease, ensuring proper surgical staging and therapy. Additionally, as photodynamic therapy (PDT) has been shown to have an application in the treatment of advanced-stage ovarian cancer,<sup>(17,18)</sup> work is underway to exchange the optical fluorophore of the tumor-targeted probe for a photosensitizing agent in order to deliver ovarian tumor-targeted intraoperative adjuvant PDT. After the removal of bulky metastases, a GSA-directed PDT agent could be administered that would be selectively internalized by ovarian cancer cells. Then, before closing the abdomen, the surgeon would shine an activating light on common sites of metastasis and organ surfaces

in order to induce the tumor-targeted agent to produce reactive oxygen species. The linkage to GSA would be anticipated to increase both the sensitivity and specificity of the photosensitizer, thereby reducing collateral damage to normal tissue produced by PDT. Thus, this tumor-targeting system could provide ovarian cancer patients with an additional strategy for the management of unresected tumor implants while minimizing side-effects.

A limitation of the present study was that we evaluated only nine cultured cell lines *in vitro* and induced *in vivo* tumor models using only four cell lines among them, and not any clinical specimens. It is possible that other cell lines of ovarian cancer might produce negative results. The successful operation of this system necessitates not only binding but also internalization of GSA into the cancer cells. Therefore, we could investigate this method only with living cells or tumors and not fixed pathological specimens. In the next step toward its clinical application, we may have to find appropriate ways to validate this method using freshly obtained surgical samples of ovarian cancer for either *in vitro* or *in vivo* animal studies.

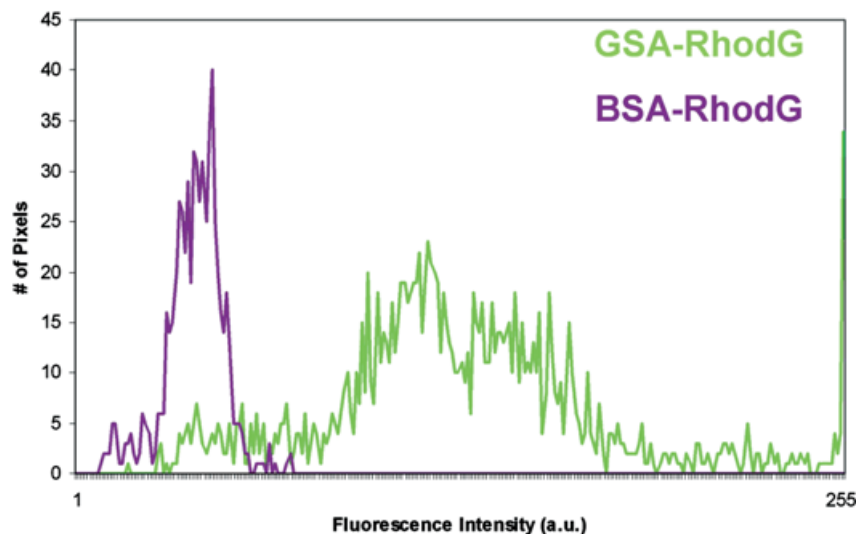
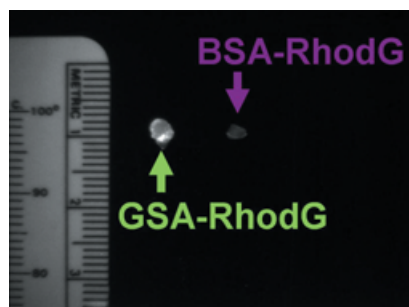


**Fig. 4.** (Top) Side-by-side *ex vivo* fluorescence image of tumor nodules derived from SKOV3 tumor-bearing mice treated with galactosyl serum albumin (GSA)-rhodamine green (RhodG) (left) and bovine serum albumin (BSA)-RhodG (right). Using ImageJ software, a region of interest was drawn around each nodule and their fluorescence intensity plotted on a histogram (bottom). Administration of GSA-RhodG resulted in higher fluorescent intensity (green line) in tumors than did BSA-RhodG administration (purple line) ( $P < 0.0001$ ). Although not shown, similar results were obtained with nodules derived from OVCAR5 and OVCAR8.

In this report, we have demonstrated that GSA-RhodG can target a wide variety of human ovarian adenocarcinomas for optical fluorescence imaging. Future studies will focus on translating these findings to the clinical setting. It is hoped that the culmination of this work will be a clinically useful targeted optical fluorophore that will be able to label metastatic ovarian adenocarcinoma implants for surgical resection, thereby improving

the completeness of cytoreductive surgery and leading to improved patient outcomes.

#### Acknowledgment

This research was supported by the Intramural Research Program of the National Institutes of Health, National Cancer Institute, Center for Cancer Research.

#### References

- Chan JK, Cheung MK, Husain A *et al.* Patterns and progress in ovarian cancer over 14 years. *Obstet Gynecol* 2006; **108**: 521–8.
- Tingulstad S, Skjeldestad FE, Halvorsen TB, Hagen B. Survival and prognostic factors in patients with ovarian cancer. *Obstet Gynecol* 2003; **101**: 885–91.
- Griffiths CT. Surgical resection of tumor bulk in the primary treatment of ovarian carcinoma. *Natl Cancer Inst Monogr* 1975; **42**: 101–4.
- Chi DS, Eisenhauer EL, Lang J *et al.* What is the optimal goal of primary cytoreductive surgery for bulky stage IIIc epithelial ovarian carcinoma (EOC)? *Gynecol Oncol* 2006; **103**: 559–64.
- Hama Y, Urano Y, Koyama Y *et al.* *In vivo* spectral fluorescence imaging of submillimeter peritoneal cancer implants using a lectin-targeted optical agent. *Neoplasia* 2006; **8**: 607–12.
- Yao Z, Zhang M, Sakahara H, Saga T, Arano Y, Konishi J. Avidin targeting of intraperitoneal tumor xenografts. *J Natl Cancer Inst* 1998; **90**: 25–9.
- Hama Y, Urano Y, Koyama Y, Choyke PL, Kobayashi H. Targeted optical imaging of cancer cells using lectin-binding BODIPY-conjugated avidin. *Biochem Biophys Res Commun* 2006; **348**: 807–13.
- Stockert RJ. The asialoglycoprotein receptor: relationships between structure, function, and expression. *Physiol Rev* 1995; **75**: 591–609.
- Hama Y, Urano Y, Koyama Y, Choyke PL, Kobayashi H. D-Galactose receptor-targeted *in vivo* spectral fluorescence imaging of peritoneal metastasis using galactosamine-conjugated serum albumin-rhodamine green. *J Biomed Opt* 2007; **XX**: XXX–XXX.
- Imai S, Kiyozuka Y, Maeda H, Noda T, Hosick HL. Establishment and characterization of a human ovarian serous cystadenocarcinoma cell line that produces the tumor markers CA-125 and tissue polypeptide antigen. *Oncology* 1990; **47**: 177–84.
- Hamilton T, Young R, Ozols R. Experimental model systems of ovarian cancer: applications to the design and evaluation of new treatment approaches. *Semin Oncol* 1984; **11**: 285–98.
- Bérnard J, Da Silva J, De Blois M *et al.* Characterization of a human ovarian adenocarcinoma line, IGR-OV1, in tissue culture and in nude mice. *Cancer Res* 1985; **45**: 4970–9.
- Hama Y, Urano Y, Koyama Y, Bernardo M, Choyke PL, Kobayashi H. A comparison of the emission efficiency of four common green fluorescence dyes after internalization into cancer cells. *Bioconjug Chem* 2006; **17**: 1426–31.
- Hytonen VP, Laitinen OH, Grapputo A *et al.* Characterization of poultry egg-white avidins and their potential as a tool in pretargeting cancer treatment. *Biochem J* 2003; **372**: 219–25.
- Paganelli G, Chinol M, Maggiolo M *et al.* The three-step pretargeting approach reduces the human anti-mouse antibody response in patients submitted to radioimmunoscintigraphy and radioimmunotherapy. *Eur J Nucl Med* 1997; **24**: 350–1.
- Kwon AH, Matsui Y, Ha-Kawa SK, Kamiyama Y. Functional hepatic volume measured by technetium-99m-galactosyl-human serum albumin liver scintigraphy: comparison between hepatocyte volume and liver volume by computed tomography. *Am J Gastroenterol* 2001; **96**: 541–6.
- DeLaney TF, Sindelar WF, Tochner Z *et al.* Phase I study of debulking surgery and photodynamic therapy for disseminated intraperitoneal tumors. *Int J Radiat Oncol Biol Phys* 1993; **25**: 445–57.
- Sindelar WF, DeLaney TF, Tochner Z *et al.* Technique of photodynamic therapy for disseminated intraperitoneal malignant neoplasms. Phase I study. *Arch Surg* 1991; **126**: 318–24.

## Supplementary materials

The following supplementary material is available for this article:

**Fig. S1.** Differential interference contrast and green fluorescence images of additional OVCAR4 cells incubated with galactosyl serum albumin–rhodamine green are shown.

**Fig. S2.** Spectral fluorescent images of two loops of the bowel and mesentery without any tumor implants 3 h after injection with 25 µg galactosyl serum albumin–rhodamine green (the same amount we used in this study) are shown. The vasculature is vaguely depicted by the rhodamine green fluorescence. No fluorescent nodule is shown on the mesentery.

**Fig. S3.** Two-color pharmacokinetic spectral fluorescence images of galactosyl serum albumin (GSA)–Cy7 (shown in green) and bovine serum albumin (BSA)–Cy5.5 (shown in red) co-injected intravenously (i.v.) (left panels: immediately and 2 min after injection) and intraperitoneally (i.p.) (right panels: immediately and 3 h after injection) are shown. Within 2 min for i.v. and 3 h for i.p., GSA–Cy7 was noted within the liver and started excreting into the biliary system, although BSA–Cy5.5 was distributed all over the body. When the fluorescent dyes for conjugation were exchanged (i.e. GSA–Cy5.5 and BSA–Cy7), the drug kinetics were unchanged. These results demonstrate that GSA was cleared quickly from the peritoneal cavity, and then accumulated and catabolized in the liver.

This material is available as part of the online article from:

<http://www.blackwell-synergy.com/doi/abs/10.1111/j.1349-7006.2007.00602.x>

(This link will take you to the article abstract).

Please note: Blackwell Publishing are not responsible for the content or functionality of any supplementary materials supplied by the authors. Any queries (other than missing material) should be directed to the corresponding author for the article.